

**Development of a wide-aperture backscattering detector (BSD)
for the HRFD diffractometer**

THEME: Development of Experimental Facilities for Condensed Matter Investigations with Beams of the IBR-2 Facility

THEME CODE: 04-4-1122-2015/2020

AUTHORS:

Kruglov V.V. - Dubna, JINR

Balagurov A.M. - Dubna, JINR

Bobrikov I.A. - Dubna, JINR

Simkin V.G. - Dubna, JINR

Bokuchava G.D. - Dubna, JINR

PROJECT LEADER Kruglov V.V.

DATE OF SUBMISSION OF PROPOSAL OF PROJECT TO SOD _____

DATE OF THE LABORATORY STC _____ DOCUMENT NUMBER _____

PROJECT ENDORSEMENT LIST

**Development of a wide-aperture backscattering detector (BSD)
for the HRFD diffractometer**

THEME: Development of Experimental Facilities for Condensed Matter Investigations with Beams of the IBR-2 Facility

THEME CODE: 04-4-1122-2015/2020

APPROVED BY JINR DIRECTOR _____ «____»_____2017

ENDORSED BY

JINR VICE-DIRECTOR _____ «____»_____2017

CHIEF SCIENTIFIC SECRETARY _____ «____»_____2017

CHIEF ENGINEER _____ «____»_____2017

HEAD OF SCIENCE ORGANIZATION
DEPARTMENT _____ «____»_____2017

LABORATORY DIRECTOR _____ «____»_____2017

LABORATORY CHIEF ENGINEER _____ «____»_____2017

PROJECT LEADER _____ «____»_____2017

ENDORSED

RESPECTIVE PAC _____ «____»_____2017

List of contents.

Introduction	4
1. International cooperation and outside organizations	4
2. Scientific case	4
2.1. Status and scientific program	4
2.2. Proposals for modernization of HRFD	5
2.3. Main characteristics of the backscattering detector	8
2.4. Detector efficiency	9
2.5. Evaluation of the geometric contribution to the total resolution of the diffractometer	10
2.6. References	11
3. Expected results and new developments.....	12
4. Competitiveness	12
5. Partner companies and equipment suppliers	12
6. Schedule of the Project	13
7. Network schedule of the Project	14
8. Estimated expenditures for the Project	15

INTRODUCTION

The High-Resolution Fourier Diffractometer (HRFD) developed in the framework of collaboration between FLNP JINR (Dubna), PNPI (Gatchina) and VTT (Espoo, Finland) has been operating at the IBR-2 reactor since 1995. Its initial design, principle of operation and nominal parameters are described in detail in [1]. Examples of numerous studies carried out with HRFD and ideas on the possible development of the diffractometer are given in [2, 3]. In the past few years, some of the key units that became morally obsolete or worn out, have been replaced. Specifically, in 2016 a new mirror neutron guide and fast Fourier chopper were put into operation and in the previous years there was a complete replacement in the data acquisition and experiment control electronics. At present, the most important element of the program for further modernization of HRFD is the replacement of existing backscattering detectors with a new version.

1. International cooperation and outside organizations

List of participants and organizations

Country or International organization	City	Contracting Institute	Participants	Status
Russia	Dubna	ATOM		Contract
Republic of Belarus	Minsk	BSU	Kuten S.A.	Protocol

2. Scientific case

2.1. Status and scientific program

Any modern high-resolution neutron diffractometer is a complex and expensive instrument, therefore precision neutron diffraction experiments with a very high resolution (at a level of $\Delta d/d \approx 0.002$ or higher) are conducted only in a few most advanced neutron laboratories in the world. At present, in Russia it can be done only at FLNP JINR (Dubna). Moreover, the HRFD diffractometer at the IBR-2 reactor is one of three or four neutron diffraction instruments in the world where it is possible to perform experiments that require the resolution $\Delta d/d \approx 0.001$ or higher. HRFD is mainly intended for **precision structural analysis of polycrystalline substances** with an average unit cell volume of up to $\sim 500 \text{ \AA}^3$. Typical examples are the studies of mercury-based high-temperature superconductors with different concentrations of oxygen or fluorine [4, 5], doped manganites with colossal magnetoresistance [6, 7], modern functional alloys and electrode materials [8, 9]. HRFD is also used to perform **analysis of single crystals** when its unique d_{hkl} resolution is needed, e.g., to study phase separation in $\text{La}_2\text{CuO}_{4+\delta}$ crystals due to low-temperature diffusion of hyperstoichiometric oxygen [10].

The layout of HRFD at the IBR-2 reactor is presented in **Fig. 1**.

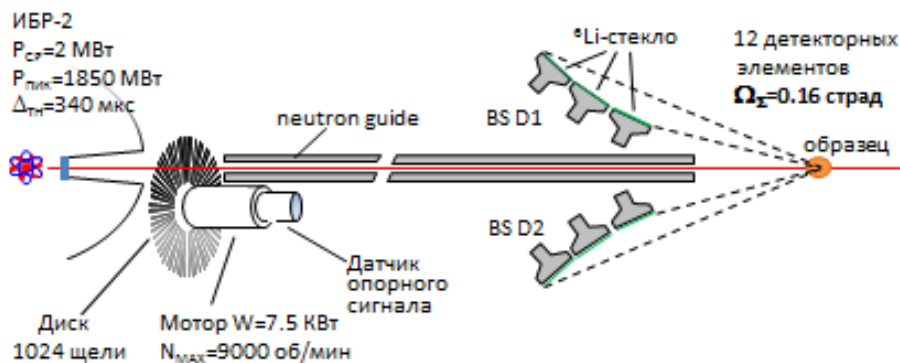


Fig. 1. Layout of HRFD at the IBR-2 reactor.

At present, the detector system of HRFD consists of three detectors, two of which are located at scattering angles of $\pm 152^\circ$, the third one is at 90° . The first two detectors are mainly used to study the structure of polycrystals, and the third one is chiefly employed for measuring internal stresses. The detecting element is Li-glass-based scintillators. From the present-day viewpoint, the HRFD detectors have two disadvantages: a high sensitivity to γ -background and an insufficiently large solid angle (~ 0.16 sr). Due to this, the resulting diffraction spectra have a rather high background and low (by modern criteria) data rate, despite the fact that the neutron flux at the sample position is sufficiently high (10^7 n/cm²/s). Thus, the diffraction spectrum obtained with the TOF diffractometer POWGEN3 (SNS/ORNL, $\Delta d/d \approx 0.001$) due to a large-area ZnS(Ag)-based detector (solid angle 1.5 sr) will have a low background and ~ 10 times better statistics than the spectrum from the same sample measured using HRFD. This project is aimed at eliminating these drawbacks. Its implementation will make it possible to radically improve the parameters of the HRFD diffractometer and bring it to the leading positions in the world. The estimates show that the solution of these problems will allow an approximately two- to three-fold increase in the number of conducted experiments, and permit us to substantially improve the accuracy of obtained structural information, as well as significantly enhance the possibilities of the diffractometer in performing experiments under various external conditions.

2.2. Proposals for modernization of HRFD

It is proposed to replace the existing backscattering detectors shown in **Fig. 1** with a new wide-aperture scintillation detector based on ZnS(Ag)/⁶LiF scintillator using combined electronic-geometric focusing.

The new detector covers the scattering angle interval $2\Theta = (133-175)^\circ$ with the corresponding total solid angle of approximately $\Omega_\Theta \approx 2.0$ sr. The technological and technical solutions used at the present time in the Laboratory make it possible to almost completely eliminate event losses due to the detector design for this solid angle. Thus, as compared to the existing detector at HRFD, the solid angle will increase by a factor of ~ 12.5 .

To ensure high and ultra-high resolution, the detector is designed on the basis of a thin 0.42-mm-thick ZnS(Ag)/⁶LiF scintillation screen. The collection and transmission of light from scintillation screens to photomultipliers are done using optical wavelength

shifting fibers. A detailed description of the features of the application of $\text{ZnS(Ag)}^6\text{LiF}$ scintillation screens is given in [11]. To illustrate the light collection scheme, **Fig. 2** shows the element of the scintillation screen together with the optical wavelength shifting fibers glued to it on both sides.



Fig. 2. Element of the scintillation screen (white plate) together with the optical wavelength shifting fibers glued to it on both sides. The curved shape of the screen is determined by the requirement of space-time focusing.

Figure 3 schematically shows the proposed version of a large-aperture detector, and **Fig. 4** – its 3D graphic presentation. The figures show only the scintillation screens and their location relative to the beam axis and the sample.

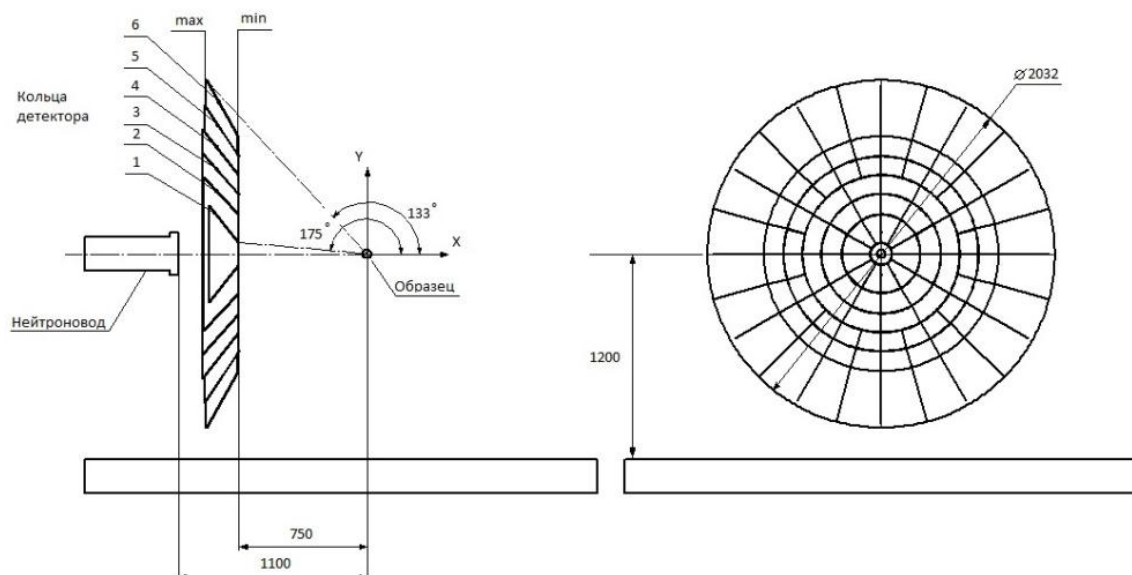


Fig. 3. Schematic of a large-aperture backscattering detector.

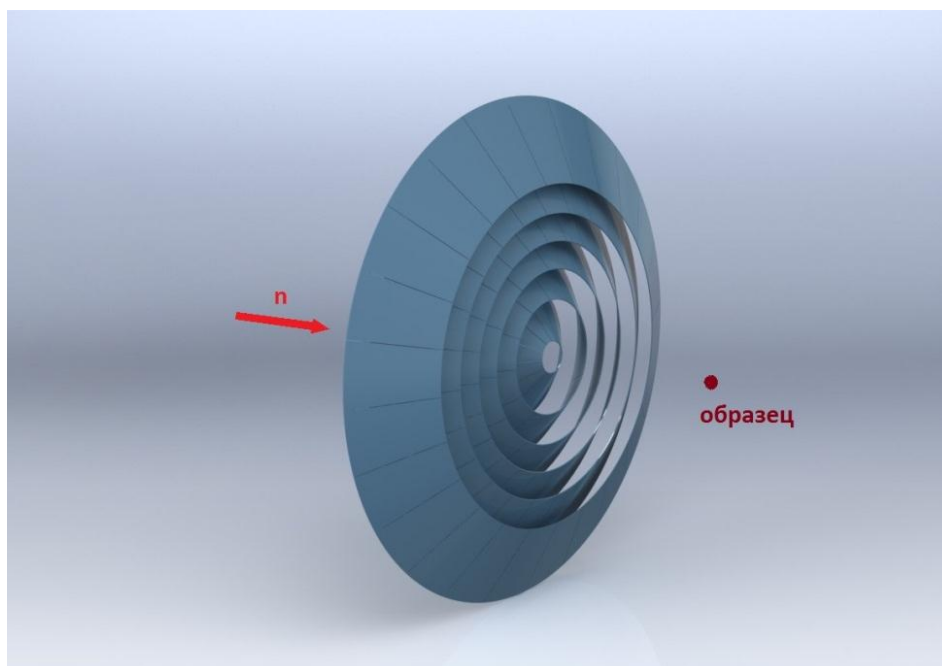


Fig. 4. 3D graphic presentation of a large-aperture backscattering detector.

It can be seen from the figure that the detector has a ring structure reflecting the axial symmetry of neutron scattering by the sample. The detector comprises 6 rings of scintillation screens. Three outer rings are divided into sectors of 15° , and three internal ones – into sectors of 30° . Six rings completely cover the scattering angle interval $2\Theta = (133-175)^\circ$. The total solid angle of the detector is $\Omega_{\Theta} \approx 2.0$ sr.

Each sector in the schematic is an independent detector element consisting of a scintillation screen, WLS fibers for light collection and a photomultiplier. A scintillation screen in each sector is not solid, but consists of smaller, tightly fitted to each other fragments which follow the surface shape of space-time focusing with the required accuracy.

The output of each photomultiplier is connected to the Data Acquisition and Accumulation System developed in the Laboratory. The description of the System is given in detail in [12]. The system allows one to receive and process information from 240 independent detectors, suppressing events caused by background gamma-rays. The System is designed in the NIM standard. In its full configuration, it consists of 8 units of amplifiers-discriminators with 32 inputs each and one data accumulation unit.

2.3. Main characteristics of the backscattering detector

The shape of the detector elements of all 6 detector rings satisfying the condition of space-time focusing is given in **Fig. 5**.

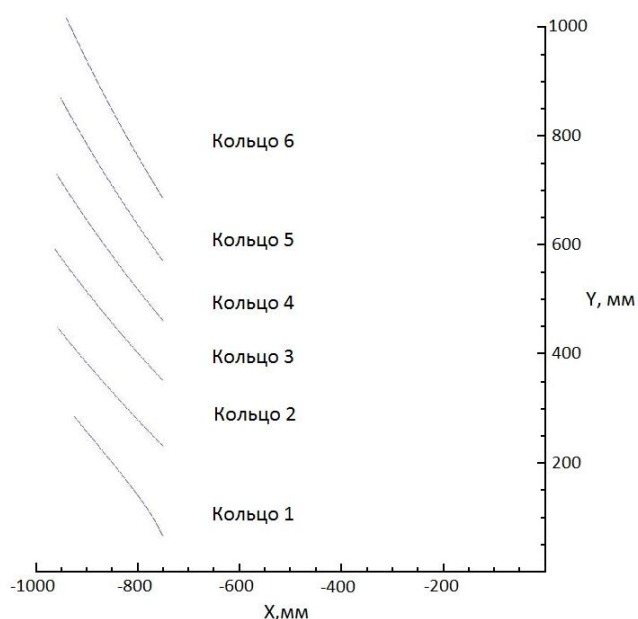


Fig. 5. Shape of the detector elements of the rings.

Table 1 presents the main geometric characteristics of the rings of the detector, providing guidance on its position at the HRFD diffractometer.

Quantity	Ring №1	Ring №2	Ring №3	Ring №4	Ring №5	Ring №6
$\theta_{max}, ^\circ$	175.047	162.913	154.917	148.417	142.721	137.547
$\theta_{min}, ^\circ$	162.913	154.917	148.417	142.721	137.547	132.745
$l, \text{ mm}$	280	300	320	340	360	380
$X_{max}, \text{ mm}$	-750.00	-750.00	-750.00	-750.00	-750.00	-750.00
$Y_{max}, \text{ mm}$	65.00	230.55	351.05	461.10	570.91	686.12
$X_{min}, \text{ mm}$	-923.44	-956.79	-961.40	-958.44	-950.62	-938.82
$Y_{min}, \text{ mm}$	283.86	447.84	591.07	729.58	869.65	1015.77
$\Delta\Omega, \text{ sr}$	0.02117	0.02627	0.02818	0.01471	0.01515	0.01547
$\Omega, \text{ sr}$	0.25388	0.31518	0.33814	0.35300	0.36360	0.37127

Table 1. Main geometric characteristics of the backscattering detector rings.

$\theta_{max}, \theta_{min}$ – maximum and minimum scattering angle, which is covered by the ring; l – length of the detector elements in **Fig. 5**; $X_{max}, X_{min}, Y_{max}, Y_{min}$ – coordinates of the end points of the scintillation screen of each ring; $\Delta\Omega$ – solid angle covered by one sector of the ring; Ω – total solid angle covered by the ring.

The dependence of the effective thickness of the detector (d_{eff}) on the scattering angle, i.e. the thickness encountered by the scattered neutron on its way from the sample, is shown in **Fig. 6**. This thickness determines both the detector efficiency, and makes a contribution to the geometric component of the diffractometer resolution. The calculations of the effective thickness have been made on the basis of the actual thickness of the scintillation screen (0.42 mm), which is optimal from the viewpoint of the balance between efficiency and transparency.

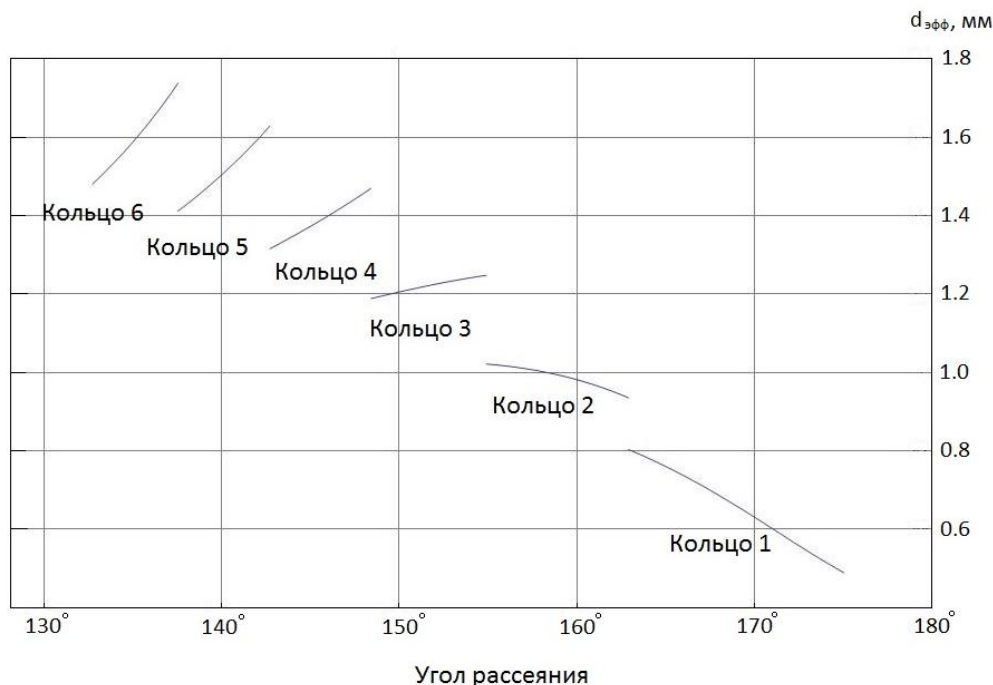


Fig. 6. Dependence of the detector effective thickness (d_{eff}) on the scattering angle. The scintillation screen thickness is 0.42 mm.

2.4. Detector efficiency

The dependence of the detector efficiency on the scattering angle, calculated on the basis of the data of **Fig. 6**, is presented in **Fig. 7**. The lower set of curves in **Fig. 7** corresponds to the standard thickness of the scintillation screen of 0.42 mm. The detector efficiency in this case varies from 36% to 80% and on average it is 65%.

To be limited to such a low efficiency, taking into account rather high complexity of the mechanical design of the backscattering detector, which is necessary to ensure high accuracy and positional stability of scintillation screens, would be highly unreasonable. The addition of a second layer of scintillator significantly changes the capabilities of the detector. As can be seen from the upper set of curves in Fig. 6, the efficiency range becomes 59%-96% and on average it increases to 85%. This increase in efficiency, combined with the aperture increased to 2 sr, will bring the backscattering detector to a completely new level. The mechanical design of the detector with the addition of the second layer remains practically unchanged.

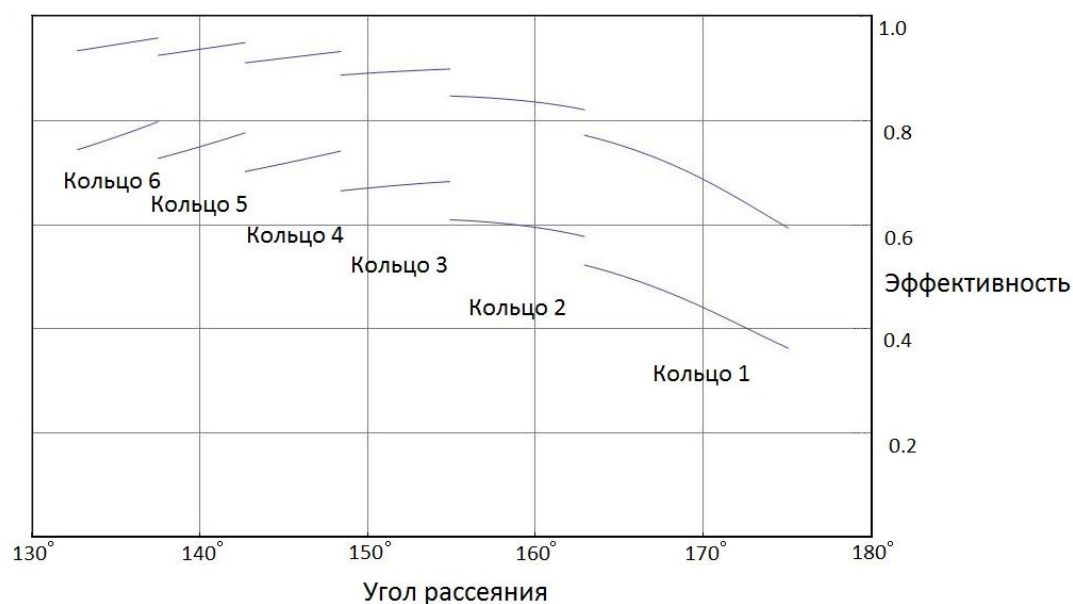


Fig. 7. Dependence of the detector efficiency on the scattering angle.

2.5. Evaluation of the geometric contribution to the total resolution of the diffractometer

The geometric contribution to the total resolution was evaluated by taking into account only the effective detector thickness and various sample sizes $\varnothing_{\text{samp}}$ ranging from 1 to 8 mm. It was assumed that the shape of the scintillation screen exactly corresponds to the shape of the time focusing surface and the initial divergence of the neutron beam is zero. The results of this evaluation are given in Table 2 which show that for the chosen detector geometry the contribution from the thickness of the scintillation screen and sample size to the diffractometer resolution is substantially below the allowable value (0.001). Technological and technical possibilities of the Laboratory make it possible to provide the shape of the screen corresponding to the time focusing surface with the required accuracy.

$\varnothing_{\text{samp}}, \text{mm}$	1	2	3	4	5	6	7	8
$\langle \Delta_1 \rangle$	4.0×10^{-5}	6.9×10^{-5}	1.0×10^{-4}	1.3×10^{-4}	1.7×10^{-4}	2.0×10^{-4}	2.3×10^{-4}	2.6×10^{-4}
$\langle \Delta_2 \rangle$	4.6×10^{-5}	7.3×10^{-5}	1.0×10^{-4}	1.3×10^{-4}	1.7×10^{-4}	2.0×10^{-4}	2.3×10^{-4}	2.6×10^{-4}
$\langle \Delta_3 \rangle$	5.1×10^{-5}	7.6×10^{-5}	1.1×10^{-4}	1.4×10^{-4}	1.7×10^{-4}	2.0×10^{-4}	2.3×10^{-4}	2.6×10^{-4}
$\langle \Delta_4 \rangle$	5.5×10^{-5}	7.9×10^{-5}	1.1×10^{-4}	1.4×10^{-4}	1.7×10^{-4}	2.0×10^{-4}	2.3×10^{-4}	2.6×10^{-4}
$\langle \Delta_5 \rangle$	5.8×10^{-5}	8.1×10^{-5}	1.1×10^{-4}	1.4×10^{-4}	1.7×10^{-4}	2.0×10^{-4}	2.3×10^{-4}	2.6×10^{-4}
$\langle \Delta_6 \rangle$	6.1×10^{-5}	8.2×10^{-5}	1.1×10^{-4}	1.4×10^{-4}	1.7×10^{-4}	2.0×10^{-4}	2.3×10^{-4}	2.6×10^{-4}

Table 2. Geometric contribution to the total resolution of the diffractometer.

$\varnothing_{\text{samp}}$ – sample size; $\langle \Delta_i \rangle = 2.36\sigma_i$ – error value for the i-th ring of the detector.

2.6. References

1. Aksenov V.L., Balagurov A.M., Simkin V.G., Bulkin A.P. et al., "Performance of the high resolution Fourier diffractometer at the IBR-2 pulsed reactor" *J. of Neutron Research*, 1997, v.5, pp. 181-200. JINR Preprint, P13-96-164, Dubna, 1996.
2. Balagurov A.M., "High resolution Fourier diffraction at the IBR-2 reactor" *Neutron News*, 16 (2005) 8-12.
3. Balagurov A.M., Kudrjashev V.A., "Correlation Fourier diffractometry for long-pulse neutron sources: a new concept" ICANS-XIX conference, 08-12.04.2010, Grindewald, Switzerland.
4. Aksenov V.L., Balagurov A.M., Sikolenko V.V., Simkin V.G. et al., "Precision neutron diffraction study of the high- T_c superconductor $\text{HgBa}_2\text{CuO}_{4+\delta}$ " *Phys. Rev. B*, 1997, v.55, pp.3966-3973.
5. Abakumov A.M., Aksenov V.L., Antipov E.V., Balagurov A.M. et al., "Effect of fluorination on the structure and superconducting properties of the Hg-1201 phase" *Phys. Rev. Lett.*, 1998, v.80(2), pp.385-388.
6. Balagurov A.M., Pomjakushin V.Yu., Sheptyakov D.V., Aksenov V.L. et al., "Effect of oxygen isotope substitution on magnetic structure of $(\text{La}_{0.25}\text{Pr}_{0.75})_{0.7}\text{Ca}_{0.3}\text{MnO}_3$ " *Phys. Rev. B*, v.60(1), 1999, pp.383-387.
7. Balagurov A.M., Pomjakushin V.Yu., Sheptyakov D.V., Aksenov V.L. et al., "A-cation size and oxygen isotope substitution effects on $(\text{La}_{1-y}\text{Pr}_y)_{0.7}\text{Ca}_{0.3}\text{MnO}_3$ structure" *Eur. Physical J. B*, 2001, v. 19 (2), pp.215-223.
8. Golovin I.S., Balagurov A.M., Palacheva V.V., Bobrikov I.A. et al., In situ neutron diffraction study of bulk phase transitions in Fe-27Ga alloys, *Materials and Design* 98 (2016) 113-119
9. Bobrikov I.A., Balagurov A.M., Chih-Wei Hu, Chih-Hao Lee et al., Structural evolution in LiFePO₄-based battery materials: in-situ and ex-situ time-of-flight neutron diffraction study, *Journal of Power Sources* 258, 356-364 (2014)
10. Balagurov A.M., Pomjakushin V.Yu., Simkin V.G., Zakharov A.A. "Neutron diffraction study of phase separation in $\text{La}_2\text{CuO}_{4+y}$ single crystals" *Physica C*, 1996, v.272, pp.277-284.
11. Kuzmin E.S., Balagurov A.M., Bokuchava G.D., Kudryashev V.A. et al., Detector for the FSD Fourier Diffractometer based on $\text{ZnS}(\text{Ag})/{}^6\text{LiF}$ Scintillation Screen and Wavelength shifting Fibers Readout. Препринт ОИЯИ Е13-2001-204.
12. Levchanovskiy F.V., Murashkevich S.M. "The Data Acquisition System for Neutron Spectrometry – a New Approach and Implementation" NEC'2013, pp.176-179.

3. Expected results and new developments

Within the framework of the project it is planned:

1. to develop a technical design of a backscattering detector (BSD) for HRFD;
2. to adapt the existing technology of manufacturing scintillation detectors for BSD at HRFD;
3. to design and manufacture instrumentation for mass production of sectors of the detector;
4. to design and manufacture the mechanical components of the detector;
5. to design and manufacture a test bench for testing detector sectors;
6. to manufacture one sector of the detector and conduct its testing on the test bench;
7. to manufacture and adjust MPD modules of detector electronics and data acquisition and accumulation electronics; to develop and debug the software.

4. Competitiveness

The detector is a unique scientific and technical development, the construction of which will bring the HRFD diffractometer to the world leaders among similar experimental instruments.

5. Partner companies and equipment suppliers:

Country or International Organization	City	Institute Contractor	Participants	Status
USA		Bicron		Contract
Japan		Hamamatsu		Contract
Russia	Dubna	SPA "Aspekt"		Contract
Italy		CAEN		Contract

Schedule proposal and resources required for the implementation of the Project

Development of a wide-aperture backscattering detector (BSD)
for the HRFD diffractometer

Main units of equipment, resources, financing sources			Costs (k\$)	Proposals of the Laboratory on the distribution of finances and resources		
				Resource requirements	2018	2019
Main units of equipment	1. Sets of photomultipliers				190	
	2. Fibers				120	
	3. Scintillator			130		
	4. Power supply				100	
	5. Data acquisition and accumulation electronics				20	20
	6. Mount fitting and consumables			50	90	90
Financing sources	Budget	Theme	810	180	520	110
Required resources	Standard hour	FLNP Experimental Workshop	500		250	250
		ATOM	1000		500	500

The cost estimate was based on a dollar/ruble exchange rate at the Central Bank of the Russian Federation as of 11.04.2017 and was 57.14 rub per 1 USD.

PROJECT LEADER

V.V.Kruglov

Network schedule of the Project
Development of a wide-aperture backscattering detector (BSD)
for the HRFD diffractometer

N		2018		2019		2020	
		I	II	I	II	I	II
1	Development of technical design of backscattering detector						
2	Manufacturing of equipment for manufacturing detector elements						
3	Purchase of equipment and consumables						
4	Construction of data acquisition and accumulation electronics (240 channels)						
5	Purchase of power supply source for systems with a large number of photomultipliers						
6	Manufacturing of detector frame and elements of detector sections						
7	Assembling of first detector section with data acquisition and accumulation systems and software						
8	Tests of first section in laboratory conditions						

Estimated expenditures for the Project
Development of a wide-aperture backscattering detector (BSD)
for the HRFD diffractometer

№	Expenditure items	Full cost	2018	2019	2020
Direct expenses for the Project					
1			-	-	
2	Design bureau				
3	Materials	k\$	165	230	20
4	Equipment	k\$	15	290	90
5	Payments for agreement-based research	k\$			
6	Travel allowance	k\$			
	a) non-rouble zone countries		8	8	8
	b) rouble zone countries		2	2	2
	c) protocol-based		-	-	
Total direct expenses		840	190	530	120

The cost estimate was based on a dollar/ruble exchange rate at the Central Bank of the Russian Federation as of 11.04.2017 and was 57.14 rub per 1 USD.

PROJECT LEADER

_____ V.V.Kruglov

« ____ » _____ 2017

FLNP DIRECTOR

_____ V.V.Shvetsov

« ____ » _____ 2017

FLNP CHIEF ECONOMIST

_____ L.S.Ovsyannikova

« ____ » _____ 2017